

A look at the utility of pulsed NMR

Katherine Magat and Vasudev Mandyam
Physics 173, Spring 2004, Prof. Kleinfeld

Introduction

Pulsed nuclear magnetic resonance (NMR) was first introduced in the 1940's by Felix Bloch and Edward Purcell. Bloch and Purcell developed methods for determining the magnetic moments of nuclei in solids and liquids. One can use pulsed NMR to identify characteristic properties of various samples. More recently, the technique of functional magnetic resonance imaging (fMRI) has contributed a lot to non-invasive brain research.

Our goal has been to use pulsed NMR to detect the difference between oxygenated and deoxygenated blood. The difference between these two blood states arises from their unique magnetic properties, which can be probed with our apparatus. Along the way, we examined glycerin and water samples as well, in order to refine our measurement techniques and learn more about NMR.

Background:

Nuclear spins. The nuclei of certain elements have a spin angular momentum,

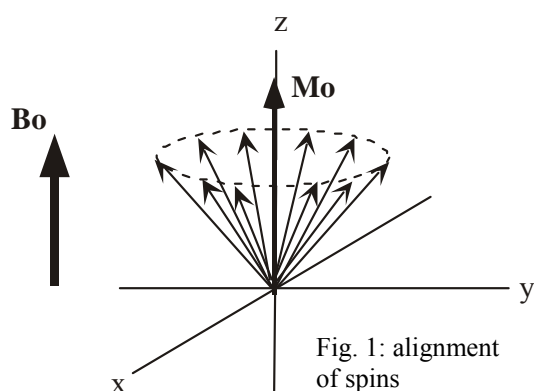


Fig. 1: alignment of spins

associated with a magnetic moment. In the presence of an external magnetic field, the orientations of the spins will either align or anti-align with the field (with a majority of the spins in the aligned state)⁵. Each orientation corresponds to a particular energy level, and NMR involves transitions between these energy levels. In our case, we are measuring the spins of water protons.

Each spin moment precesses around the axis of the magnetic field (see Fig. 1). The frequency of precession, called the Larmour

frequency, is proportional to the strength of the field:

$$f = \gamma B_0$$

where γ is the gyromagnetic ratio of the material, and B_0 is the static field strength.

Resonance. A resonance condition occurs when there is an RF-field applied transverse to the static field at the precession frequency. The transient field will rotate the ensemble of magnetic moments away from the static field axis. The static field is assumed to be in the z-direction; the pulsed field thus rotates the magnetization into the xy-plane (see Fig. 2)³.

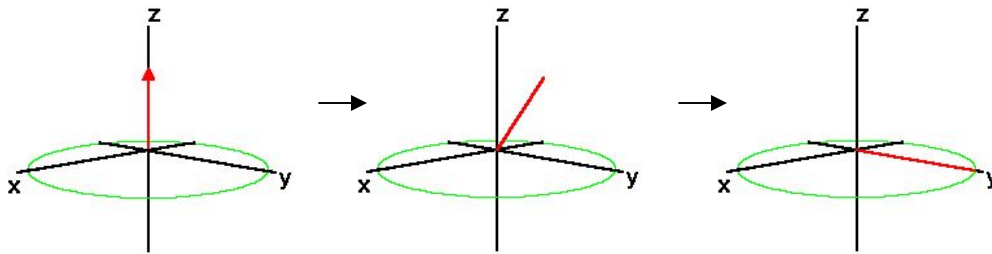


Fig. 2: Upon application of an RF pulse, net magnetization is knocked out of the z-axis and gains a component in the xy-direction.

Free Induction Decay. With the absorption of the RF energy, the population of nuclei in the equilibrium state decreases while the population in the higher energy state increases, until a saturation level is reached. The magnetization vector, now lying in the xy-plane, quickly spreads out and decays due to longitudinal and transverse relaxation effects (to be discussed later). When looking at a signal after an RF-pulse, one observes this decay,

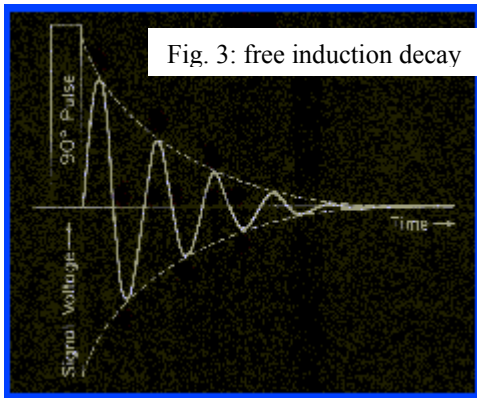


Fig. 3: free induction decay

known as the free induction decay or FID (see Fig. 3).

We speak of delivering RF “pulses” to the system. These are short bursts of RF energy, which rotate the spins by a certain amount away from the z-axis. For instance, a 90° -pulse will “knock” the spins from the z-direction into the xy-plane. A 180° -pulse will knock the spins all the way to the $-z$ direction. The spins will then begin to decay back to their original orientation. The pulse’s angle is determined by its duration—a

180° -pulse is thus twice as long as a 90° -pulse.

There are two relaxation processes involved in spin decay: the longitudinal, or spin-lattice relaxation and the transverse, or spin-spin relaxation. First, in longitudinal relaxation, the z-component of the magnetization exponentially decays to its equilibrium value with characteristic time constant T_1 (see Fig. 4)³.

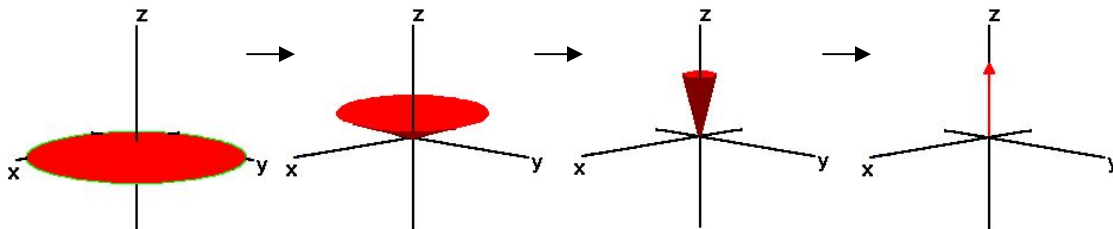


Fig. 4: T_1 relaxation. The magnetization moment (shown as being spread out over the entire xy-plane) decays back to its original orientation along the z-direction.

Transverse relaxation refers to the exponential decay of the xy-component of the net magnetic moment, and is characterized by time constant T_2 . There are actually two sub-

processes at work in T2—namely T2-inhomogeneous and T2-pure (T2-pure is often just called T2). These add to form T2*:

$$1/T2^* = 1/T2\text{-pure} + 1/T2\text{-inhomogeneous}$$

(Note that an FID results from a combination of T2* and T1 effects). T2-inhomogeneous arises from local inhomogeneities in the static B-field. Once the spins have been knocked away from the z-axis, they begin to precess with a given frequency. However, some moments experience different local field strengths due to an imperfect field, and thus precess faster or slower than others. The net result is that the spins “de-phase” and spread apart in the xy-plane. T2-inhomogeneous is the dominant effect.

The pure T2 effect takes a lot longer than the inhomogeneous one, and is a result of random molecular interactions. These break up the alignment of the spins, also causing a net de-phasing in the xy-plane (see Fig. 5)³.

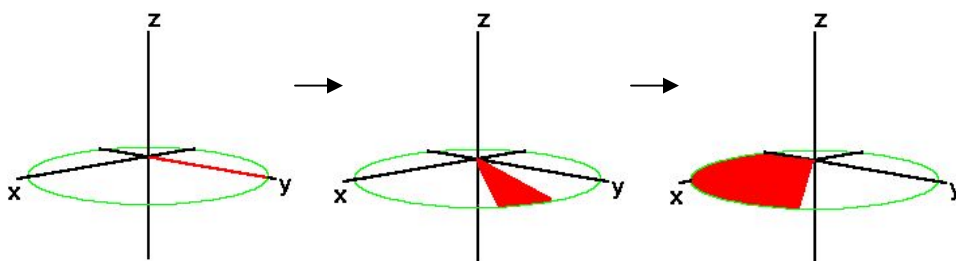
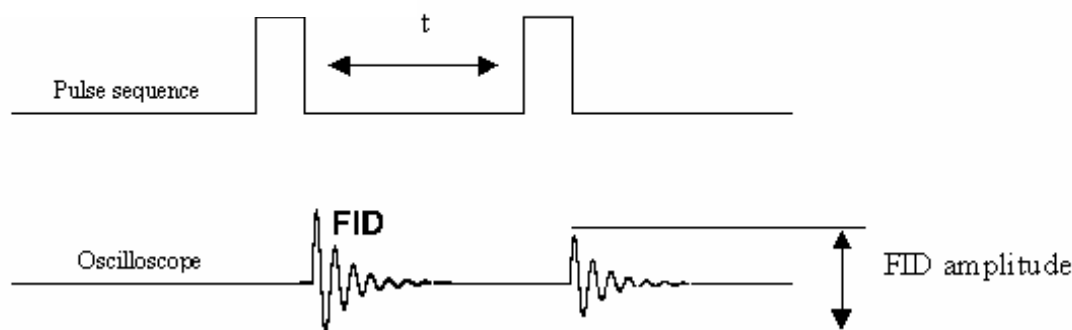


Fig. 5: de-phasing of magnetization in the xy-plane, which is the T2 effect.

Now we can look at how these relaxation times are measured. T1 measurement uses a 90-90 pulse sequence as seen in the following figure:

Fig. 6: Pulse sequence for T1



Two 90°-pulses are delivered in succession. The first pulse kicks the spins into the xy-plane, after which they begin to decay. The second pulse rotates them another 90 degrees, leaving only a small xy-component remaining. One can measure the FID amplitude of the second pulse as a function of the time between pulses. Notice that the FID will approach a maximum value with longer and longer delay times.

Measuring T2 is slightly more complicated. In order to eliminate T2-inhomogeneous, one uses the “spin-echo” technique (Figs. 6,7)³. Here a 90°-pulse knocks the spins into the xy-plane, at which point they start to de-phase. After a certain

time t , a 180° -pulse rotates all the spins over, keeping them in the xy -plane. Spins that were precessing faster are now behind of the rest, and spins that were precessing slower are now ahead of the rest. Therefore, after an equivalent time t , the spins will all “catch up” to each other, creating a large signal, called the spin-echo. We measure this echo as a function of the time between the pulses, giving us a value for T_2 .

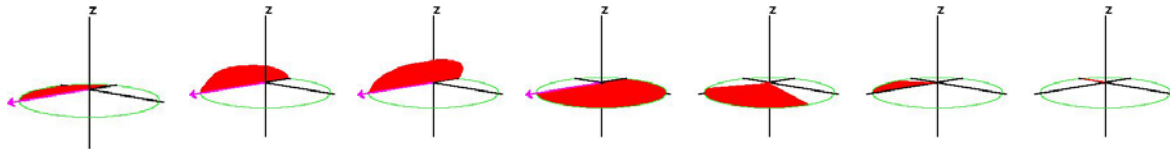
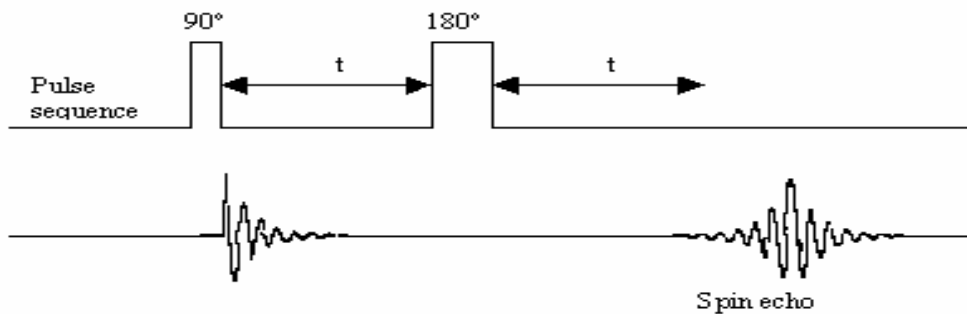


Fig. 6: Diagram of de-phased magnetization undergoing 180° -pulse and then re-phasing.

Fig. 7: Pulse sequence for T_2



Diffusion. Typically, T_1 and T_2 are first-order exponential graphs of the form

$$Y = A + B \cdot \exp(-t/T)$$

However, in the case of less viscous fluids such as water, diffusion causes additional effects⁶. Over the course of a measurement, a given water proton will move within the sample, thus experiencing different local field strengths. This causes a change in precession frequency and thus a change in the signal. To compensate for this, one can introduce a cubic term into the equation:

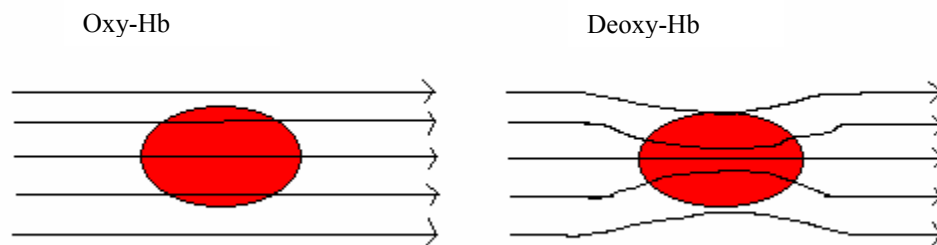
$$Y = A + B \cdot \exp(-t/T - \gamma^2 G^2 D t^3 / 12)$$

where G is the field gradient (Tesla/meter) and D is the diffusion constant (m^2/second).

Blood and the BOLD effect¹. The goal of these measurements is to detect a difference between oxygenated and deoxygenated blood. The reason for this contrast is the different magnetization states of hemoglobin (Hb). Oxy-Hb is diamagnetic, while deoxy-Hb is paramagnetic. Diamagnetic hemoglobin has little effect on the spins of water protons in the blood. However, in deoxygenated blood, as water protons diffuse across red blood cells, they pass by local paramagnetic centers, which enhance the local field that the proton sees (see Fig. 8). This effectively shortens the relaxation time of deoxy-blood.

The difference between the two times is called the BOLD (blood oxygenation level dependent) effect.

Fig 8: effects of oxygenation state on magnetic field



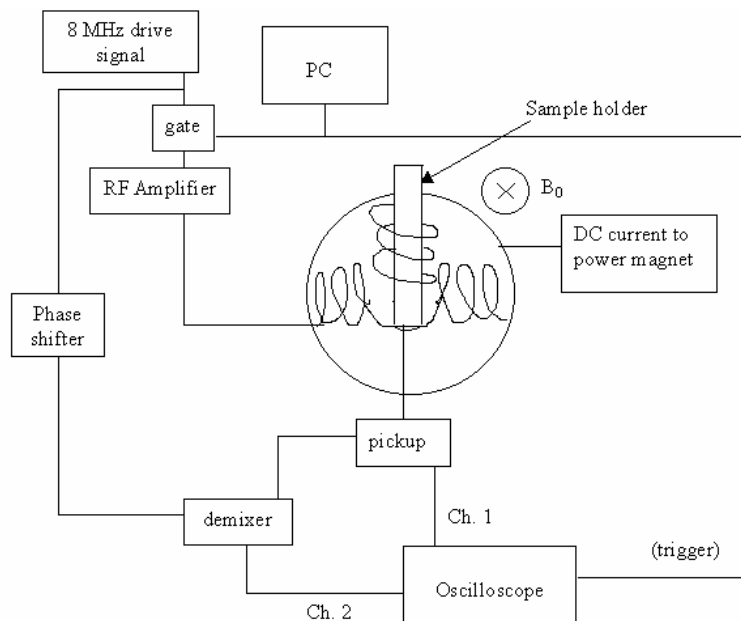
a) A red blood cell containing oxygenated (diamagnetic) Hb has no effect on magnetic fields passing through and around it.

b) A red blood cell with deoxygenated (paramagnetic) Hb causes local variations in the magnetic field.

Materials and Methods:

Materials and setup. A “home-made” pulsed NMR apparatus already present in the laboratory was used to make all the measurements. See Fig. 9 for a diagram of the setup.

Fig 9: Pulsed NMR measurement apparatus.



The setup consists of a signal generator set to deliver an 8 MHz signal. This signal passes through a computer-controlled gate that delivers pulses, and is amplified before heading to the sample.

The sample is placed into a small holder located in the middle of a large magnet with field strength $B_0=0.2$ T, pointed in the z-direction, powered by a DC current source (which can be tuned to adjust the field strength).

Wrapped around the sample holder are two sets of orthogonal coils: a drive coil and a pickup coil, both perpendicular to B_0 . The pickup coil's signal goes to the oscilloscope, where one can see things such as the FID and spin-echo from the sample. Also, the pickup coil is mixed with the raw signal in a de-mixer, which then passes to the oscilloscope. This raw signal first passes through a phase-shifter, which allows for more

precise tuning of the signal to resonance. Then, the de-mixed signal extracts the envelope of the FID and echo, allowing us to use averaging to obtain more precise measurements.

Samples measured. Three different substances were tested in our experiment: glycerin, water, and blood. The samples were all placed in a small Vacutainer (a vacuum-sealed test tube used for storing blood samples), which was roughly half-filled. Glycerin was readily available in the lab. Tap water was used for the H₂O samples. For the whole blood samples, fresh human blood was drawn from Katherine and Vasudev.

Preparation of the blood involved oxygenation and deoxygenation. To oxygenate the blood, two open needles were punched through the top of the vacutainer. A very slight vacuum was drawn on one of the needles, so that there was a constant airflow across the top of the blood inside the tube, allowing it to oxygenate.

Deoxygenation involved two different methods. The first was to blow compressed nitrogen gas across the surface of the blood. The second, which is the method of choice in the data presented here, is to add a small pinch of sodium dithionite (Na₂S₂O₄), a reducing agent which automatically deoxygenates the blood.

Methods and measurements. T1 and T2 relaxation times were the focus of all our measurements. These measurements require delivery of a gated RF pulse of specified duration. Pulse duration is determined by examining the free induction decay (FID) amplitude on the oscilloscope. When the FID is at its largest, this duration corresponds to a 90° pulse, as all the spins are in the plane of the pickup coil. A 180° pulse duration is twice that of a 90° pulse, and corresponds to a minimum FID. Our measurements were further optimized by fine-adjustment of the DC current of the static magnet. This allows for precise matching of the field strength with the corresponding Larmour frequency.

The T1 pulse sequence consists of two 90° pulses delivered in sequence (see Background section for theory). The second FID amplitude is measured as a function of the time between the two pulses. We used the demixed signal and varied the phase to maintain the signal shape throughout our measurements—this allows us to see the optimum signal for each given data point. Fitting the curve to an exponential decay gives us the characteristic time constant T1.

For measuring T2, we used a 90-180 pulse sequence. The spin-echo amplitude is measured as a function of the time from the first pulse to the spin echo. Fitting the curve to an exponential decay gives the characteristic time constant T2.

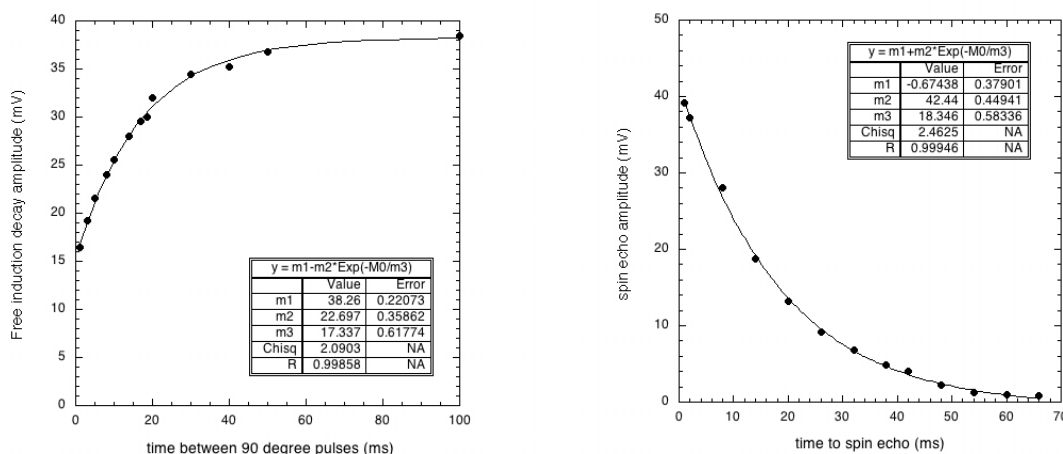
Finally, we made a rough measurement of the field gradient over the region in which the sample tube lies inside the magnet. This allows for comparison with the gradient calculated from the diffusion of water. Using glycerin as our sample, we used a thin tube (roughly 1/3 the diameter of the vacutainer), and moved the tube to different locations within the sample holder. By adjusting the drive frequency of the signal generator to optimize the spin-echo seen, we could effectively determine the gradient in the static magnetic field (recall that $f = \gamma B_0$).

Results:

Glycerin yielded very good data for T1 and T2 times, as shown in Fig. 10 below. The T1 data was fitted to an exponential curve of the form $y=A-B*\text{Exp}(-t/T1)$. As seen in the figure, the FID amplitude increases to a maximum as the delay between pulses increases. We found a spin-lattice relaxation time of $T1=17$ ms.

Similarly, our T2 data was fitted to the equation $y=A+B*\text{Exp}(-t/T2)$, the difference here arising from the fact that as pulse delay increases, the spin-echo signal decreases. We found a spin-spin relaxation time of $T2=18$ ms.

Fig. 10: Glycerin



a) FID amplitude versus pulse delay, yielding T1 relaxation curve for glycerin. Data fits to a first-order exponential.

b) Spin-echo amplitude versus time to spin echo, yielding T2 relaxation curve for glycerin, fitted to a first-order exponential.

Next, we measured the relaxation times of water, as seen in Fig. 11. We used a different fit here, due to the high diffusion constant of water (see Background). It is an exponential equation with a cubic term, which goes as

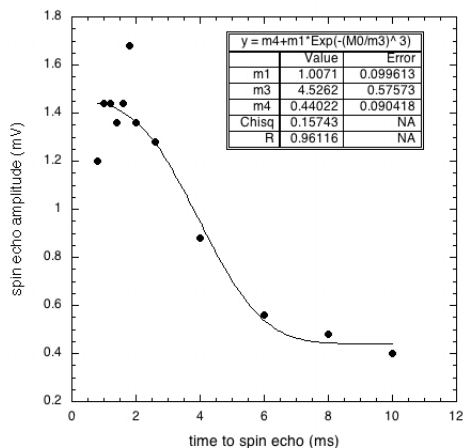


Fig. 11: T2 relaxation data for H₂O.

$$Y = A + B * \text{Exp}((-t/\alpha)^3)$$

$$\text{where } \alpha = \frac{12}{\gamma^2 G^2 D}$$

From the exponential fit, we see that $\alpha = 4.53 * 10^{-3} \text{ sec}^{-3}$.

The gyromagnetic ratio $\gamma = 4.2574 * 10^7 \text{ Hz/Tesla}$.

The diffusion constant has a value of $D=22 \text{ m}^2/\text{s}$ at room temperature.

Finally, Fig. 12 shows data collected for oxygenated and deoxygenated blood. The data sets were not fit with any equations, as they do not seem to follow the expected exponential pattern. We do see that deoxygenated blood has a quicker spin-echo decay than does oxygenated blood. No conclusions can be made with certainty as to relaxation times—however, more shall be mentioned in the following section.

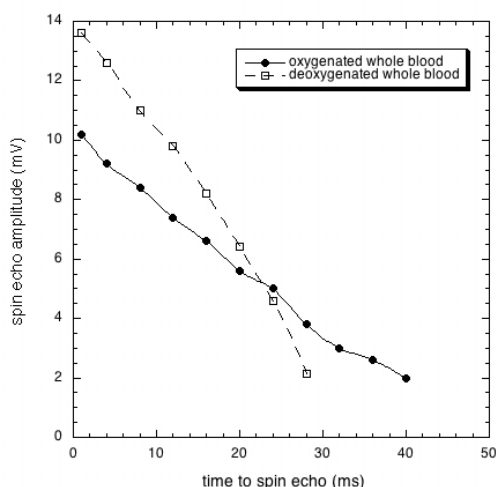
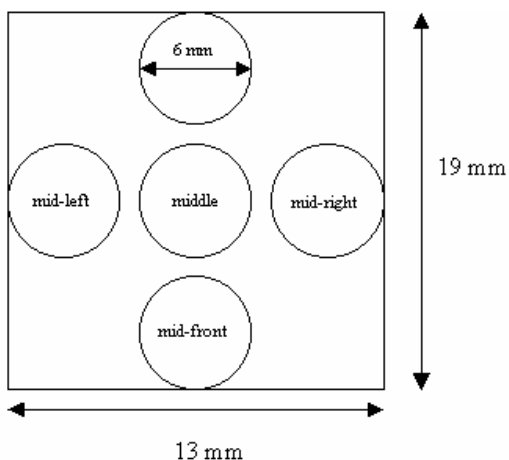


Fig. 12: Plot of spin echo amplitude versus time from first pulse to spin echo, for oxygenated and deoxygenated whole blood.

The field gradient and sample holder looked as follows (not to scale):



Here is our raw data of drive frequency as a function of position over the sample holder:

<u>Position</u>	<u>Frequency (MHz)</u>
Middle-left	8.000
Middle-right	7.996
Middle	7.996
Middle-front	7.992
Middle-back	7.995

Fig. 13: top-down view of the sample holder.

Calculations and Discussion:

Glycerin has proved to be a reliable sample for pulsed NMR testing—this is why we chose it to examine the field gradients as well. For both T1 and T2 measurements, our data fit the expected exponential curves quite well. This is most likely because

glycerin is much more viscous than water or blood, thus reducing any effects that diffusion might introduce. Our values agree with other independent measurements⁴.

The water data emphasizes the effects of diffusion on measurements of less viscous fluids. The very high diffusion constant of water (22 m²/s) indicates that a water molecule can move a large distance over the timescale of a measurement, which is on the order of microseconds. Note that the full equation of fit has both a first-order time term and a cubic time term, while in our data we only used the cubic term. This is because the cubic term dominates the fit, making the t-term itself negligible. From the fitted parameters of the modified equation, we calculated the field gradient by solving for G:

$$G^2 = \frac{12}{\gamma^2 D \alpha^3} \rightarrow G = 5.69 \cdot 10^{-5} \text{ T/m}$$

We can also calculate our field gradient measured by varying the drive frequency. First, all the frequencies are converted into B-field strengths using the precession equation. Then, we can simply find the difference between middle-left and middle-right field strengths and divide by the corresponding distance to find the side-to-side gradient. The same calculation will also yield the front-to-back gradient. We find that

$$G_{\text{side-to-side}} = 0.0143 \text{ T/m}$$

$$G_{\text{front-to-back}} = 0.0231 \text{ T/m}$$

This gradient is significantly larger than the one found using the water fit. We trust this latter calculation more, simply because it was a more direct approach. Rather than using a fit parameter to find G, we actually measured it. These gradients are decently large enough to affect our experiments, and they must therefore be accounted for.

Finally we move on to the results gathered from whole blood. The expected results would have been two exponential curves with different T2 times, such that one can discern oxygenated from deoxygenated blood. While this did not occur in our data, we nevertheless see a trend. Consistent with current literature, deoxygenated blood shows a quicker spin-echo decay than oxygenated blood¹. Both exhibit decays on the order of tens of milliseconds, with deoxy-blood falling off faster.

There are several possible reasons that we cannot be more conclusive about our results. First and foremost was our weak magnetic field. It has been found that T2 depends quadratically on the static field strength². This means a very strong field, on the order of several Tesla, creates long T2 times, making the absolute difference between oxy- and deoxy-T2 much larger. In our case, however, the weak field of roughly 0.2 T makes it quite difficult to discern a difference. Secondly, our coil setup was not shielded and oriented very well, causing the pickup coil to receive stray signals from the drive coil and external field (where it should only be sensing changes in the sample).

All in all, while our data was not entirely conclusive for blood, we are quite pleased with the results. They serve as a good foundation for future pulsed NMR experimentation.

Acknowledgements

Thanks to Tyson Kim for his masterful phlebotomy skills and his time. Thanks also to Chris Schaffer for his wisdom and guidance in virtually every single aspect of this class. Finally, thanks to Earl Dolnick for helping with our setup and materials.

References

1. Ogawa, S., Lee, T. M., Kay, A. R., and Tank, D. W. (1990) *Biophysics*. Vol. 87, pp. 9868-9872.
2. Thulborn, K., Waterton, J., Matthews, P., and Radda, G. (1982) *Biochimica et Biophysica Acta*. Vol. 714, pp. 265-270.
3. Hornak, J.P. *The Basics of NMR*. <http://www.cis.rit.edu/htbooks/nmr/>, 6/9/2004.
4. Frazier, Rob. *The Measurement of Relaxation Times in Mineral Oil and Glycerin Using Pulsed Nuclear Magnetic Resonance*. <http://frazier.home.cern.ch/frazier>, 6/9/2004.
5. Gauthier, Jeff. "Pulsed NMR." Physics 173/273, Spring 2003, Prof. Kleinfeld, University of California, San Diego.
6. Physics 4803 L (Advanced Physics Lab) manual. *Pulsed Nuclear Magnetic Resonance*. <http://www.phys.ufl.edu/courses/phy4803L/nmr/nmr.pdf>. Dept. of Physics at the University of Florida, Spring 2004.